STUDIA UBB CHEMIA, LXVI, 2, 2021 (p. 287-297)
(RECOMMENDED CITATION)
DOI:10.24193/subbchem.2021.2.25

PREPARATION AND CHARACTERIZATION OF ATORVASTATIN-LOADED POLYVINYLPIRROLIDONE-BASED ELECTROSPUN MICROFIBROUS MATS

EMŐKE RÉDAI[a], IZABELLA RÁDULY[a], ZOLTÁN-ISTVÁN SZABÓ[b], ADRIANA CIURBA[a], NICOLETA TODORAN[a], PAULA ANTONOAEA[a]*, ROBERT-ALEXANDRU VLAD[a], PÉTERFI ORSOLYA[a], EMESE SIPOS[b]

ABSTRACT. The aim of this experimental work was the enhancement of water solubility of the lipid lowering drug, atorvastatin, by embedding it in polymer based micro-sized fibers, prepared by electrospinning. Characterization of the fibrous mats included morphological investigations, determination of drug content, disintegration time, small volume dissolution- and DSC studies. The electrospinning process was continuous without droplet formation. The obtained fibers were homogenous, continuous filaments with smooth surfaces. Average fiber diameters were slightly above 1 μm, while disintegration of fiber mats upon contact with water was almost instantaneous (three to ten seconds). Dissolution of the lipid lowering drug was almost complete, when using a solution feed rate of 1 mL/h.

Keywords: *atorvastatin, electrospinning, PVP, microfibrous mats*

INTRODUCTION

The first-line lipid lowering drug, atorvastatin (AT), is a synthetic HMG-CoA reductase inhibitor, which acts mainly by reducing low-density lipoprotein cholesterol levels. It is widely used for the treatment of hypercholesterolemia, effectively reducing morbidity and mortality in patients with atherosclerosis. Benefic effects appear also in patients with normal LDL-cholesterol levels. By

[a] *„George Emil Palade" University of Medicine, Pharmacy, Sciences and Technology of Targu Mures, Faculty of Pharmacy, Pharmaceutical Technology and cosmetology department, Gh. Marinescu street no. 38, 540142 Targu Mures, Romania*
[b] *„George Emil Palade" University of Medicine, Pharmacy, Sciences and Technology of Targu Mures, Faculty of Pharmacy, Pharmaceutical Industry and Management department, Gh. Marinescu street no. 38, 540142 Targu Mures, Romania,*
** Corresponding author: paula.antonoaea@umfst.ro*

inhibiting the cholesterol pathway, atorvastatin also possesses anti-inflammatory effects (1, 2). Although the drug of choice in hyperlipidemia, atorvastatin has a low oral bioavailability (around 12%), which increases its dose (3). According to Biopharmaceutical Drug Classification System (BCS) atorvastatin belongs to class II, possessing low solubility and good permeability (4). In case of BCS class II, solubility is the rate limiting step in oral absorption and solubility enhancing techniques are promising ways to increase bioavailability (5).

One of the greatest challenges in pharmaceutical formulations development is solubility enhancement of poorly water-soluble drugs. Various techniques have been recommended to increase bioavailability, among these are procedures which increase solubility by incorporating the drug in highly hydrophilic polymers (6). Electrospun fiber mats are produced from viscous polymeric solutions, under a high electric field. The benefits of these nano - or microfibrous systems include high surface area-to-volume ratios, high porosity and the possibility of stabilizing the active ingredient in an amorphous state (7) verified by thermal methods (8). Important progresses were also made in the industrial scale-up of the process, hopefully opening the gate to greater acceptance of the method in the pharmaceutical industry also (9).

There are some studies, which address the poor physicochemical properties of AT and other statins, in most of the cases, with the aid of nanotechnology. AT has been incorporated in polyvinyl pyrrolidone K30 based electrospun solid dispersions by Jahangiri et collaborators (10). Chitosan nanoparticles obtained by ionic gelation proved to ensure sustained release of atorvastatin (11). The anti-inflammatory effect of AT containing inclusion complex embedded in a polycaprolactone-based membrane was demonstrated by Schwinte (12). AT coated controlled-release stents (13-15), and also fibers for peripheral nerve injury in rats (16, 17) were also studied. Rosuvastatin fibers with heparin were also embedded in endovascular stents (18-20). Simvastatin fiber mats for bone tissue regeneration (21, 22) including healing of femoral defect (23) were formulated. A poloxamer-based lovastatin nanofibrous formulation was also prepared in order to improve the chemical stability of the drug (24).

Jahangari et al. prepared amorphous dispersions of AT, using PVP K30 (25). The authors prepared methanolic solutions with different ATV:PVP ratios and prepared solid dispersions by the solvent evaporation technique, using a rotavapor. AT was present in an amorphous form in the prepared solid dispersion, which resulted in improved dissolution rate of the active. Moreover, the total cholesterol and LDL cholesterol levels decreased significantly more, when AT was administered in the form of solid dispersions, when compared to the physical mixture.

In a follow-up study, Jahangari et al. (10) presented the preparation and physicochemical evaluation amorphous nano-solid dispersions atorvastatin, either alone or in combination with ezetimibe. In this case, solid dispersions were prepared by electrospraying using PVP K30 as an amorphous carrier. The electrospraying solutions were prepared by dissolving the appropriate amount of the active substance and PVP in methanol:acetone 1:1 (v/v) with drug:polymer concentrations of 10% and 20%. The obtained nano-solid dispersions were characterized by high surface area and contained the active substances in an amorphous state, which lead to higher dissolution rates.

Recently, Iqbal et al. (26) reported the preparation of AT and metformin containing PVP and/or hyaluronic acid-based nanoparticles (either with or without polysorbate 20). Electrospraying was performed on solutions prepared in ethanol:methanol 1:1 (v/v) and the authors achieved around 4% AT drug-load in the prepared formulations. The prepared nanoparticles provided enhanced dissolution rate and higher oral bioavailability for the active substances as compared to the marketed products.

As it can be observed there is a great interest in the preparation of AT containing solid dispersions as it offers an efficient way to increase the solubility, dissolution rate of the active, which in terms can translate into an increase of bioavailability of the lipid-lowering drug. Nano- or microfibrous formulations were yet to be applied for immediate-release AT formulations. In the present study, we aim to describe the incorporation of AT in amorphous form into PVP-based microfibers for solubility and dissolution rate enhancement of the active ingredient. Tracking of physicochemical changes during electrospinning was also aimed as well as characterization of the obtained fibrous mats, including morphological investigations, drug content, disintegration time, dissolution and thermal studies.

RESULTS AND DISCUSSION

In the present study, AT was incorporated into electrospun microfibrous meshes, in order to present a novel, greener platform for the dissolution enhancement of the lipid lowering blockbuster drug. As the lower molecular weight PVP K30 proved to be an excellent choice for preparing AT-containing solid dispersions in previous studies (10, 25-26). Being an inert, pH-stable, biodegradable hydrophilic, amorphous polymer, which displays a complex affinity for both hydrophilic and hydrophobic drugs (27) it represents an excellent choice for the carrier matrix of AT. Moreover, PVP solutions in alcohol-type solvents are easily electrospinnable and the active substances

incorporated in these PVP-based nano- or microfibrous products show increased solubility and enhanced dissolution rate. Thus, in order to increase the solubility of AT, PVP was chosen as a hydrophilic polymer and microfibrous samples could be obtained by electrospinning the prepared viscous solutions. Morphology and diameters of the fibrous samples were determined by a simple optical microscopic approach, calibrated with a standard scale. The obtained fibers were homogenous, continuous filaments with smooth surfaces. The electrospinning process was continuous and droplet formation was not observed. All of the examined samples presented average fiber diameters slightly above 1 μm (being significantly different $P < 0.0001$, by one way Anova test) with relatively narrow individual fiber diameter distributions (Table 1 and Figure 1). The authors are unaware of previously described immediate-release electrospun fibrous formulations of AT, however, the observed fiber diameters are in-line with earlier reported microfibrous formulations of the poorly soluble fenofibrate, prepared by electrospinning ethanolic PVP-based viscous polymeric solutions (28).

Table 1. Summary of the results obtained during the characterization of the microfibrous samples

Batch	***Flow rate (ml/h)***	***Diameters of fibers (μm*** ±SD***)***	***Disintegration time (seconds)***	***Drug content (%w/w*** ±SD***)***	***Dissolved AT after 30 minutes (%w/w*** ±SD***)***
ATV		-	-	-	38.34 ±1.12
I.	0.5	1.381 ± 0.37	5	11.67 ± 0.45	69.29 ±0.28
II.	1	1.335 ± 0.28	4	11.25 ± 0.56	99.21 ±4.02
III.	3	1.059 ± 0.20	3	11.92 ± 0.12	86.31 ±1.21
IV.	4	1.415 ± 0.37	10	12.46 ± 0.70	71.03 ±0.32

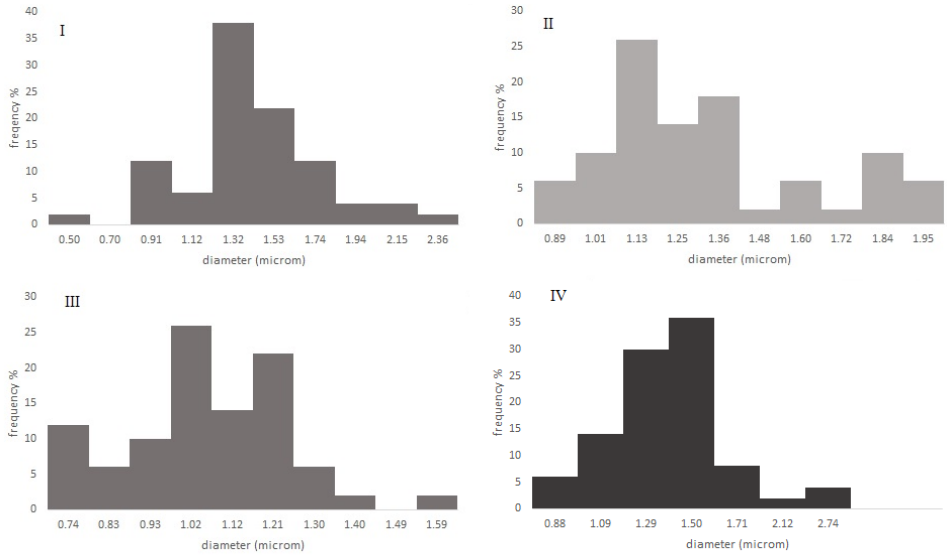

Figure 1. Diameter distribution by image analysis for the different formulations.

A representative image of the obtained fibers is presented in Figure 2.

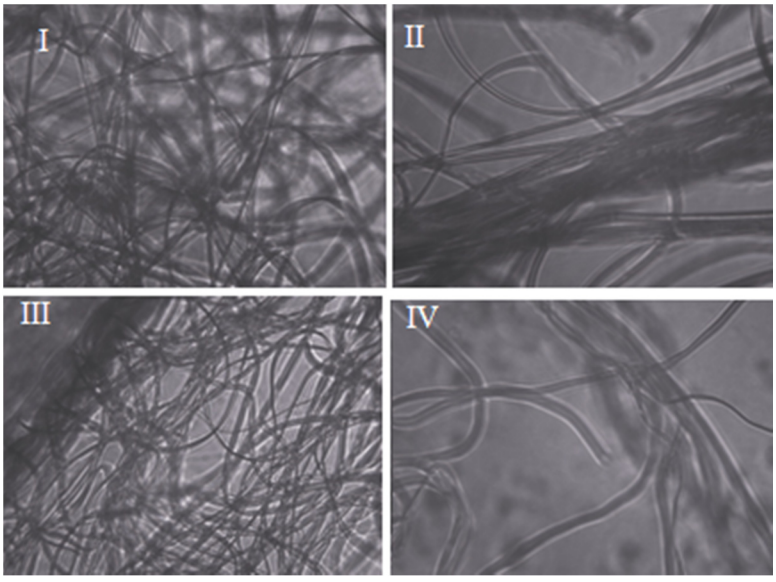

Figure 2. Microscopic images of atorvastatin electospun fibers for batches I-IV (40x)

Using a hydrophilic polymer of lower molecular weight enhances the disintegration of the obtained fiber mats, upon contact with water (29). Moreover, the highly porous structure and high surface area-to-volume ratio can further decrease the disintegration time. Indeed, the obtained fibrous structure disintegrated rapidly in a few seconds, releasing the active ingredient, when in contact with water.

Electrospinning offers an efficient method for incorporation of various small molecules or biomacromolecules in diverse polymeric matrices. Compared to other nanocarrier systems, electrospinning can offer higher drug loading or entrapment efficiency (30). The drug content of the fibers varies between 11.25 and 12.46 % w/w, which is adequate, considering that an average dose of 20 mg AT could be delivered in around 160-180 mg microfibrous mesh.

Incorporation in a solid carrier structure enhanced the dissolution rate compared to pure active substance (Figure 3). An almost complete dissolution was achieved, when a feed rate of 1mL/h was used. A feed rate of 3 mL/h was associated with 86.31% AT dissolved. Lowest feed rate showed the lowest amount of AT liberated after 30 minutes. Dissolution rate and fiber size is influenced by flow rate (31). Lowest fiber size (1.059 μm) was obtained at a feed rate of 3 mL/h and was associated with the rapidest disintegration.

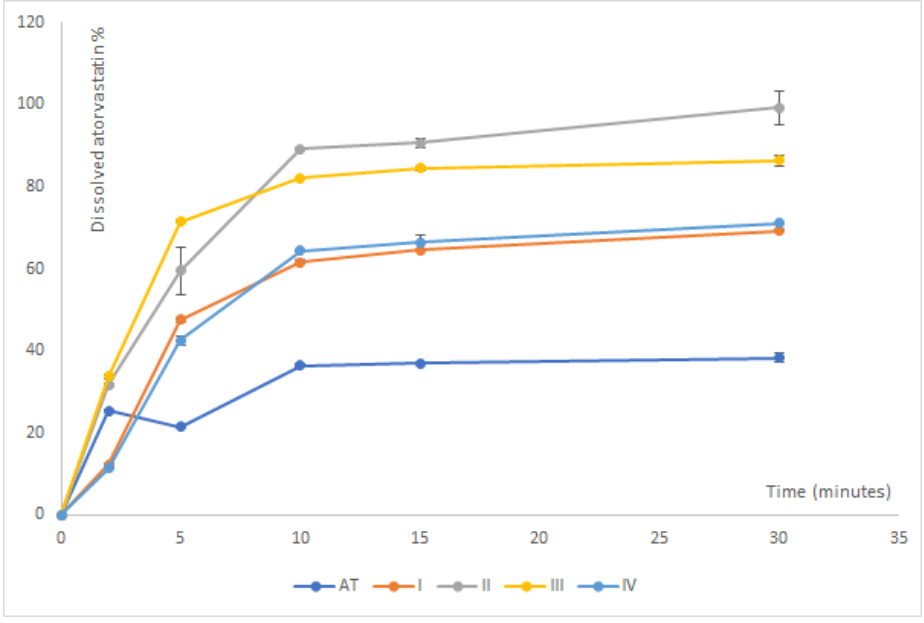

Figure 3. Dissolution curves of the pure drug and samples.

Setting the optimal flow rate for the electrospinning process mainly depends on the volatility of the solvents used and the applied electric field. Higher flow rates should be used in order to compensate for the rapid evaporation of highly volatile solvents and the applied electric field should be high enough to ensure the extraction of the polymer jet from the nozzle tip (30). Generally, using flow rates higher the optimal value, would result in thicker fibers and/or bead formation or sometimes in high residual solvent concentration in the deposited fibers (30). In our case, fiber diameter decreased with increasing the feed rate of the polymeric solution, up until a 3mL/h optimum value was attained. However, a further increase in feed rate resulted in increased fiber diameter, most probably due to thicker jet formation.

The thermogram of pure atorvastatin presents an endothermic heat exchange at 162°C, characteristic of the melting of the crystalline active substance (32). The DSC curve of Plasdone K-29/32 shows an endothermic event below 100°C, characteristic for the dehydration of the polymer. The melting endotherm of AT disappears from the DSC curve of fibrous samples and no enthalpy change is detectable, which could be due to the amorphization of active ingredient. Figure 4 presents the recorded DSC curves. The possibility of inducing the crystalline-to-amorphous transition of the incorporated active substances is often exploited during the immediate release formulations prepared through electrospinning. The formation of an amorphous solid dispersion is favored by electrospinning, due to the rapid solvent evaporation and due to the limited time available for drug crystallization during the process (30).

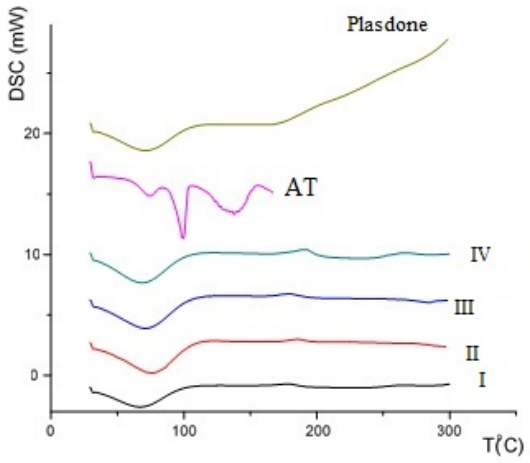

Figure 4. DSC curves of the pure drug and samples.

CONCLUSIONS

AT microfibers were prepared by electrospinning from PVP-based viscous solutions. The obtained fiber mats prepared from the hydrophilic, low molecular weight PVP and presented almost instantaneous disintegration, when in contact with water, rapidly releasing AT. Incorporation of the poorly soluble lipid-lowering blockbuster drug in the polymeric fibers through electrospinning, induces a possible crystalline to amorphous transition of the active, increasing the dissolution rate and solubility of AT.

EXPERIMENTAL SECTION

Materials

AT calcium trihydrate was a kind gift of Morepen Laboratories, New Delhi, India; Polyvinylpyrrolidone K value 29 to 32 (Plasdone K/29-32) was from Gaf Chemicals USP; methanol and ethanol were obtained from Chemical Company, Iasi, Romania; sodium dihydrogen phosphate monohydrate was obtained from Merck, Darmstadt, Germany; potassium dihydrogen phosphate was obtained from Loba Chemie, Austria.

Methods

Preparation of the viscous polymeric solution for electrospinning

The solutions used for electrospinning were prepared by dissolving 0.25 g AT in 3.0 g methanol under stirring using a JKI SMS HS magnetic stirrer (JKI, Shanghai, China). Then, 4.25 g ethanol and 2.5 g Plasdone K-29/32 was added. Stirring continued for another 15 minutes. A homogeneous viscous solution was obtained.

Preparation of atorvastatin fibers by electrospinning

Atorvastatin-loaded fibrous sheets were prepared by electrospinning using an in-house assembled apparatus. The flow rate was set to 0.5, 1, 3 and 4 ml/h (Batch I, II III and IV - using an Ascor AP12 infusion pump) and the voltage 25 kV. The syringe was connected to a size 21 G (0.8 mm external diameter) metallic needle with silicone tube. Fibers were collected on a grounded static sheet covered with aluminum foil after a 10 cm flight.

Morphology investigation by microscopy

Fiber morphology was tracked using a Bresser LCD Micro 5 MP microscope (Bresser, Rhede, Germany) at 40x magnification. Recorder images were examined with ImageJ software (US National Institutes of Health, Bethesda, MD, USA). Finally, the average diameter of nanofibers was calculated using 50 different randomly selected individual filaments.

Differential scanning calorimetry (DSC)

Thermal analysis was performed using a Shimadzu Thermo Analyzer DSC 60 (Shimadzu, Tokyo, Japan) equipment. Samples of 5 mg were accurately measured. Scans were performed at a heating rate of 5°C/min and using a temperature range of 30-300°C in not-hermetically sealed aluminum pans in air atmosphere.

Determination of disintegration time

5 mg of fibrous sheets were introduced in 10 ml distilled water at room temperature, and the disintegration time was measured.

Determination of drug content of atorvastatin microfibers

Drug content was determined using 25 mg fibers (dissolved in 20 ml methyl alcohol and distillated water) with a Dionex Ultimate 3000 system (Dionex, Olten, Switzerland) using a reversed-phase high-performance liquid chromatography method. Chromatographic separation was realized with a Phenomenex Luna C18, 250x4.6 mm column as stationary phase, at a temperature of 40°C. Mobile phase consisted of 1% aqueous acetic acid 1% and acetonitrile. Gradient elution was used, employing a 15 minutes linear gradient from 5 % to 95 % of acetonitrile delivered at a flow rate 1 ml/min. Injection volume was 25 µl. Detection was performed at 244 nm.

Small volume dissolution studies

Small volume dissolution studies were performed with an in-house assembled dissolution setup, which consisted of 11.5 cm long glass tubes immersed in a water bath maintained at 37 ± 1°C, using an Erweka ET 1500I thermostat (Erweka GmbH, Heusenstamm, Germany) (33). Stirring was realized with a 10x2 mm Teflon-coated stirring bar with a magnetic stirrer (Intop AB69, Wenzhou Start Co. Ltd, China) at a speed of 75 rpm. Dissolution media was 10 ml phosphate buffer at pH 6.8. Samples of 1 ml were taken at predefined intervals (2, 5, 10, 15, 30 minutes), filtered through a 0.45 µm filter and assayed with the previously described method. Determinations were performed in triplicate.

ACKNOWLEDGMENTS

Research funded by project 84.2/2017/P.2/EMEOGYSZ.

REFERENCES

1. A.R. Pradeep; M. Kumari; N.S. Rao; S.S. Martande; S.B. Naik; *J. Periodontology*, **2013**, *84*, 871-879
2. J. Li; J.-J. Li; J.-G. He; J.-l. Nan; Y.-l. Guo; C.-M. Xiong; *Cardiovascular Therapeutics,* **2010**, *28*, 8-14
3. M.A. Shaker; H. M. Elbadawy; S. S. Al Thagfan; M.A. Shaker; *Int J Pharm,* **2021**, *592*, 120077
4. S. Kumar; D. Bhargava; A. Thakkar; S. Arora **2013**, *30*, 217-256
5. P. Pandi, R. Bulusu, N. Kommineni, W. Khan, M. Singh, *Int J Pharm*, **2020**, *586*, 119560
6. P. Khadka; J. Ro; H. Kim; I. Kim; J.T. Kim; H. Kim; J.M. Cho; G. Yun; J. Lee, *Asian J Pharm. Sci.*, **2014**, *9*, 304-316
7. I. Sebe; P. Szabó; B. Kállai-Szabó; R. Zelkó; *Int J Pharm*, **2015**, *494*, 516-530
8. P. Antonoaea; N. Todoran; A. Rusu; A. Ciurba; M. Birsan; E. Redai; *Revista de Chimie*, **2018**, *69(12),* 3692-3697
9. P. Vass; E. Szabó; A. Domokos; E. Hirsch; D. Galata; B. Farkas; B. Démuth; S. K. Andersen; T. Vigh; G. Verreck; G. Marosi; Z.K. Nagy; *WIREs Nanomed. Nanobiotechnol.*, **2020**, *12*, e1611.
10. A. Jahangiri; M. Barzegar-Jalali; Y. Javadzadeh; H. Hamishehkar; K. Adibkia; *Artificial Cells; Nanomed. Biotechnol.*; **2017**, *45*, 1138-1145
11. V.J.B; B. Madhusudhan; *Int J Pharm and Bio Sci*, **2015**, *6*, P50-P58
12. P. Schwinte; A. Mariotte; P. Anand; L. Keller; Y. Idoux-Gillet; O. Huck; F. Fioretti; H. Tenenbaum; P. Georgel; W. Wenzel; S. Irusta; N. Benkirane-Jessel; *Nanomedicine,* **2017**; *12*; 2651-2674
13. J. Chu; L. Chen; Z. Mo; G.L. Bowlin; B.A. Minden-Birkenmaier; Y. Morsi; A. Aldalbahi; M. El-Newehy; W. Wang; X. Mo; *Acta Biomat*; **2020**
14. J. Chu; L. Chen; Z. Mo; A. Aldalbahi; M. El-Newehy; W. Wang; X. Mo; 3539225.
15. C.-H. Lee; M.-J. Hsieh; S.-C. Liu; J.-K. Chen; S.-J. Liu; I. C. Hsieh; M.-S. Wen; K.-C. Hung; *Materials Sci. Eng.*: C; **2018**; *88*; 61-69.
16. M.K. Haidar; S.S. Timur; A. Kazanci; O.F. Turkoglu; R.N. Gürsoy; E. Nemutlu; M.F. Sargon; E. Bodur; M. Gök; K. Ulubayram; *Eur J Pharm Biopharm***, 2020**
17. A. Kazanci; F. Turkoglu; N. Gürsoy; E. Nemutlu; F. Sargon; E. Bodur; M. Gök; K. Ulubayram; L. Öner; H. Eroğlu; *Eur J Pharm Biopharm*; **2020**
18. M. Janjic; F. Pappa; V. Karagkiozaki; C. Gitas; K. Ktenidis S. Logothetidis; *Int J of Nanomed*, **2017**, *12*, 6343
19. C.-H. Lee; S.-H. Chang; Y.-H. Lin; S.-J. Liu; C.-J. Wang; M.-Y. Hsu; K.-C. Hung; Y.-H. Yeh; W.-J. Chen; I.-C. Hsieh; *Biomat*; **2014**, *35*, 4417-4427

20. P. Liu; Y. Liu; P. Li; Y. Zhou; Y. Song; Y. Shi; W. Feng; X. Mo; H. Gao; Q. An; *ACS Appl. Mat. Interfaces*, **2018**, *10*; 41012-41018
21. A.I. Rezk; T.I. Hwang; J.Y. Kim; J.Y. Lee; C.H. Park; C.S. Kim; *Mat Lett*, **2019**, *240*, 25-29
22. M. Kouhi; M. Morshed; J. Varshosaz; M.H. Fathi; *Chem Eng J*.; **2013**, *228,* 1057-1065
23. M. Hajializade; M. Moghtadaei; A. Mirzaei; S. Abdollahi; P. Babaheidarian; H. Pazoki-Toroudi; A. Yeganeh; *Mat Sci Eng C,* **2020**, 110861
24. S. Kajdič; Š. Zupančič; R. Roškar; P. Kocbek; *Int J Pharm,* **2020;** *573*; 118809
25. A. Jahangiriab; M. Barzegar-Jalalia; A. Garjanid; Y. Javadzadehc; H. Hamishehkara; A. Afroozianad; K. Adibkiaa; *Pow Technol*, **2015**, *286*; 538-545
26. R. Iqbal; O. Salman Qureshi; A.M. Yousaf; S.A. Raza; H.S. Sarwar; G. Shahnaz; U. Saleem; M.F. Sohai; *Eur J Pharm Sci,* **2021**, *181;* 105817
27. M. Kurakulaa; G.S.N. Koteswara Rao*; J Drug Deliv Sci Technol*, **2020**, *60*; 102046
28. E. Sipos; T. Csatári; A. Kazsoki; A. Gergely; E. Bitay, Z.I. Szabó; R. Zelkó; *Pharmaceutics*, **2020**, *12(7)*, 612
29. Z.K. Nagy; K. Nyúl; I. Wagner; K. Molnár; G. Marosi; *Express polymer letters,* **2010**, *4*, 763-772
30. J. Pelipenko; P. Kocbek; J. Kristl; *Int J Pharm*, **2015**, *484*, 57-74
31. P.R. Vuddanda; A.P. Mathew; S. Velaga; *Reactive Functional Polymers*, **2016**, *99*, 65-72
32. C. Tizaoui; H. Galai; M. Barrio; S. Clevers; N. Couvrat; V. Dupray; G. Coquerel; J.-L. Tamarit; I. B. Rietveld; *Eur J Pharm Sci*, **2020**, *148,* 105334
33. E. Sipos; Z.I. Szabó; E. Rédai; P. Szabó; I. Sebe, R. Zelkó; *J Pharm Biomed Anal,* **2016**, *129*, 224-228